

Miniband effects on hot-electron photoluminescence polarization in GaAs/AlAs superlattices

V. F. Sapega, V. I. Perel', A. Yu. Dobin, D. N. Mirlin, and I. A. Akimov
A. F. Ioffe Physico-Technical Institute, Russian Academy of Sciences, 194021 St. Petersburg, Russia

T. Ruf, M. Cardona, and K. Eberl
Max-Planck-Institut für Festkörperforschung, Heisenbergstraße 1, D-70569 Stuttgart, Federal Republic of Germany
 (Received 15 October 1996; revised manuscript received 14 March 1997)

We have studied the polarization properties of the hot electron photoluminescence (HEL) in GaAs/AlAs superlattices (SL's) and found that they are strongly affected by electron miniband formation. The quasi-three-dimensional motion of the SL electrons results in a dependence of the HEL polarization on their ratio of lateral and miniband kinetic energy. We discuss the effect of a magnetic field on the linear HEL polarization in the Faraday and Voigt geometries. Measurements in the Voigt geometry clearly demonstrate that the momentum distribution of photogenerated electrons is strongly anisotropic. The photogenerated electrons propagate predominantly along the SL growth direction when their kinetic energy is smaller than the electron miniband width or comparable to it. However, when their kinetic energy exceeds the miniband width electrons with lateral momenta dominate in the momentum distribution function. We present a theory of the HEL polarization in SL's and its magnetic field dependence which explains these observations. [S0163-1829(97)04935-7]

I. INTRODUCTION

The absorption of linearly polarized light in GaAs-type semiconductors leads to the alignment of the crystal momentum of photogenerated electrons while excitation by circularly polarized light results in a spin orientation of the excited electrons. Thus the hot electron luminescence (HEL) can be (partially) linearly or circularly polarized¹⁻³ when oriented carriers recombine with equilibrium holes.

This effect results from the selection rules for optical interband transitions. The radiative recombination of electrons with wave vector $\mathbf{K}=(k_x, k_y, k_z)$ is linearly polarized. The intensity of the radiation with polarization \mathbf{e}_{lum} emitted by the electron when recombining with a heavy hole can be represented by¹

$$I(\mathbf{e}_{\text{lum}}, \mathbf{K}) = I_0(|\mathbf{K}|) \left[1 - \frac{(\mathbf{e}_{\text{lum}} \cdot \mathbf{K})^2}{|\mathbf{K}|^2} \right], \quad (1)$$

where the polarization vector \mathbf{e}_{lum} is a unit vector parallel to the electric field of the light. The degree of linear polarization of radiation propagating along the z direction is defined as

$$\rho_l = (I_x - I_y)/(I_x + I_y),$$

where I_x and I_y refer to the intensities of the light with polarization vector \mathbf{e}_{lum} along the x and y axes, respectively. Using Eq. (1) one can obtain the degree of HEL polarization for electrons with wave vector \mathbf{K} recombining with a heavy hole:

$$\rho_{l\mathbf{K}} = \frac{k_y^2 - k_x^2}{k_x^2 + k_y^2 + 2k_z^2}. \quad (2)$$

Under excitation with linearly polarized light the momentum distribution function becomes anisotropic. This fact, in ac-

cordance with Eq. (2), leads to the linear polarization of the HEL. The initial angular dependence of the momentum distribution function $F(\mathbf{K})$ of electrons excited by linearly polarized light from the heavy-hole subband to the conduction band can be given in a form analogous to Eq. (1) if \mathbf{e}_{lum} is substituted by \mathbf{e}_{exc} :

$$F(\mathbf{K}) \propto \frac{k_y^2 + k_z^2}{k_x^2 + k_y^2 + k_z^2}. \quad (3)$$

The properties of the HEL polarization have been studied in detail for bulk GaAs and InP.¹⁻³ It was demonstrated that the linear polarization has only a weak dependence on the electron kinetic energy. Similar effects have been observed recently in GaAs/AlAs-type multiple quantum wells⁴⁻⁹ (MQW's) and were considered theoretically in Ref. 10. The main feature of the HEL polarization in the 2D case, as compared to the bulk, is its strong dependence on the initial electron kinetic energy. The linear polarization in a QW varies from $\rho_l=0$ at zero lateral kinetic energy up to of $\rho_l \sim 0.5$ at kinetic energies exceeding the confinement energy.

The dependence of the polarization on the kinetic energy in a QW can be qualitatively obtained from Eqs. (2) and (3). In order to apply these relations to the $1 \text{ hh} \rightarrow 1 \text{ e}$ transition between the first hole (1 hh) and electron (1 e) subbands it is necessary to substitute k_z^2 by the mean square of k_z in the first confined state: $\langle k_z^2 \rangle \sim (\pi/L)^2 \sim 2m_c E_1/\hbar^2$, where L is the QW width, m_c the electron effective mass, and E_1 the electron confinement energy. After this substitution Eq. (3) becomes

$$F(\mathbf{k}) \propto F_0 [1 + \alpha \cos(2\varphi)],$$

where

$$\alpha = -\frac{k^2}{k^2 + 2\langle k_z^2 \rangle}, \quad (4)$$

$$F_0 = \frac{k^2 + 2\langle k_z^2 \rangle}{2(k^2 + \langle k_z^2 \rangle)}.$$

In these equations $\mathbf{k}=(k_x, k_y)$ is the lateral (2D) wave vector, φ the angle between \mathbf{k} and \mathbf{e}_{exc} , and α the so-called alignment factor.⁴ We assume here and below that the z axis as well as the propagation direction of the exciting and photoluminescence light are perpendicular to the QW plane. It can be seen from Eqs. (2) and (4) that $\rho_{\text{LK}}=\alpha=0$ at $k=0$. Thus the polarization of the HEL is absent if the lateral energy is zero and increases as the latter increases, as experimentally observed.⁹ A rigorous theoretical study,⁴ taking into account the heavy- and light-hole mixing, slightly modifies the dependence of the linear polarization on the electron energy expressed in Eqs. (2) and (4).

Circularly polarized excitation in GaAs-type semiconductors results in an optical orientation of the electron spins and circularly polarized recombination radiation.¹⁻³ In bulk GaAs the circular polarization ρ_c of the HEL, defined analogously to ρ_l , depends weakly on the electron kinetic energy. In QWs the circular polarization ρ_c depends strongly on the lateral wave vector varying from the maximum value at $k=0$ down to zero at $k \geq \pi/L$.^{9,10}

In a magnetic field B the Lorentz force rotates the electron momenta. In the Faraday geometry, i.e., for B and the propagation direction of the exciting light parallel to each other and to the QW growth direction, the effects of the magnetic field on the linear polarization are similar in bulk semiconductors and QW's: The magnetic field leads to the depolarization of the HEL. However, in the Voigt geometry (direction of the exciting light perpendicular to B which is in the QW plane) the magnetic field effect on the linear polarization differs drastically for bulk materials and QW's: In the bulk the HEL is depolarized by a magnetic field whereas in a QW the polarization does not depend on B as long as the confinement energy exceeds the cyclotron energy of the electrons.⁶

In this work we investigate the effect of miniband formation, i.e., the intermediate region between the two limits realized in the bulk and in QWs, on the HEL polarization properties of GaAs/AIAs superlattices (SL's), both with and without a magnetic field. Preliminary results have been reported in Refs. 12 and 13. In a SL, constituting a quasi-three-dimensional system, we find polarization properties which are different compared to those of QW's (2D case) and the bulk. We perform tight binding calculations which correctly reproduce the experimental results. We demonstrate that polarized HEL can be used to measure the SL miniband width and propose a method for the optical generation of electrons with a momentum distribution function elongated either in the SL growth direction or perpendicular to it, i.e., momentum-selective optical alignment, depending on excitation energy. This may be helpful for the study of hot electron transport in SL's.

TABLE I. Parameters of the GaAs/AIAs SL and MQW samples used in the HEL experiments.

Sample	GaAs (Å)	AIAs (Å)	Doping (10^{18} cm^{-3})
40/6	39	6	1.0
40/14	38	14	1.3
40/80	40	80	0.7

II. EXPERIMENT

The SL and MQW samples investigated were grown by molecular-beam epitaxy on (001)-oriented undoped semi-insulating GaAs substrates. The central regions of the GaAs wells ($\approx 15 \text{ \AA}$ thick) were doped with Be, while the sides of these layers ($\approx 12 \text{ \AA}$ thick) were left undoped. The sample parameters, listed in Table I, were determined by double-crystal x-ray diffraction, using Cu $K\alpha_1$ radiation, and by Hall-effect measurements. The samples consist of 60 periods.

For HEL excitation we used different dye lasers pumped by an Ar-ion laser as well as He-Ne and Kr-ion lasers. The laser power density focused on the sample was $10 - 15 \text{ W cm}^{-2}$. The samples were mounted in an optical exchange-gas cryostat and kept at a temperature of 6 K. The HEL was analyzed by a SPEX 1404 or a DFS-24 double monochromator, equipped with a cooled GaAs photomultiplier and conventional photon-counting electronics. The experiments were carried out in magnetic fields up to 7 T in the back-scattering Faraday or Voigt geometries with the propagation direction of incident and scattered light normal to the (001) plane of the sample, i.e., parallel to the growth direction.

III. EXPERIMENTAL RESULTS AND DISCUSSION

A. The linear polarization of the HEL

HEL spectra in p -doped SL's at low temperatures are due to recombination of hot electrons with acceptor-bound holes (i.e., $1 \text{ hh} \rightarrow 1e \rightarrow A^0$ type transitions). Under excitation of moderate intensity (in our experiment the density of photo-created carriers was about 10^9 cm^{-2}) the main mechanism of electron energy relaxation is the emission of LO phonons. Thus the spectra of all samples show oscillations with a well resolved zero-phonon peak which reveals the initial energy distribution of photocreated electrons and LO-phonon replicas corresponding to energy relaxation via subsequent LO-phonon emission.

All spectra were excited with either linearly or circularly polarized light. The electric field vector of the exciting laser \mathbf{e}_{exc} was parallel to the $[110]$ axis of the sample. To describe the linear polarization we use the notation $\rho_l = (I_{\parallel} - I_{\perp}) / (I_{\parallel} + I_{\perp})$, where I_{\parallel} and I_{\perp} are the luminescence intensities measured in the same polarization as the exciting light ($\mathbf{e}_{\text{lum}} \parallel \mathbf{e}_{\text{exc}}$) or perpendicular to it ($\mathbf{e}_{\text{lum}} \perp \mathbf{e}_{\text{exc}}$), respectively. In the Voigt geometry we measured also linearly polarized HEL under circularly polarized excitation. In this case I_{\parallel} and I_{\perp} denote intensities measured for the polarization axis of the emitted light parallel or perpendicular to \mathbf{B} , respectively. To express the degree of circular polarization we use the similar expression $\rho_c = (I_+ - I_-) / (I_+ + I_-)$, where I_+ and I_- are HEL intensities polarized like the ex-

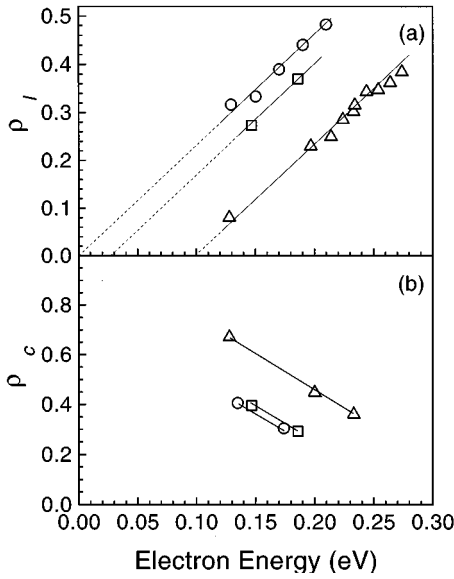


FIG. 1. Dependence of the linear ρ_l (a) and circular ρ_c (b) polarizations of the zero-phonon HEL peak maximum on the hot electron kinetic energy E in a (40/80) Å GaAs/AlAs MQW (circles) and two SL's with (40/14) Å (squares) and (40/6) Å (triangles) well and barrier widths, respectively. The lines are guides to the eye.

citing light or opposite to it, respectively. The circular polarizations are defined with respect to a fixed laboratory coordinate system and do not depend on the propagation direction of the light.

1. Energy-dependence of the linear polarization at the HEL zero-phonon peak maximum

The dependence of the HEL polarization on electron kinetic energy was measured at the maximum of the zero-phonon peak. Figure 1(a) shows the dependence of the linear polarization ρ_l on the hot electron kinetic energy ($\mathbf{e}_{\text{exc}} \parallel [110]$) for three samples with barrier widths of 6 Å, 14 Å, and 80 Å and a well width of $L=40$ Å. To calculate the electron kinetic energy E we used the relation $E = \hbar\omega_{\text{lum}} - (E_g - E_A)$, where $\hbar\omega_{\text{lum}}$ is the energy of the HEL zero-phonon peak, E_g is the band gap energy of the SL, and E_A is the acceptor binding energy. The value of $E_g - E_A$ is the experimentally measured energy of the edge luminescence. The dependence of ρ_l on E for the (40/80) Å sample [circles in Fig. 1(a)] coincides with that measured in a MQW,⁹ i.e., it approaches zero when E goes to zero. In the case of the (40/14) Å and (40/6) Å SL's [squares and triangles in Fig. 1(a), respectively] ρ_l depends on the barrier width and tends to zero for $E=27$ meV and 100 meV, respectively. Figure 1(b) displays the dependence of the circular polarization ρ_c on E in the same samples.

These peculiarities of the energy dependence of the polarization in SL's can be understood with the help of Fig. 2 which shows schematically the relevant optical transitions in a SL. The excitation of electrons in the first electron miniband takes place from the first heavy-hole subband (1 $hh \rightarrow 1e$). For the sake of simplicity we take the heavy-hole miniband width equal to zero. The total kinetic energy E of these electrons is the sum of their lateral kinetic energy E_k and the miniband energy E_Q : $E = E_k + E_Q$ [see Eq. (A2) in

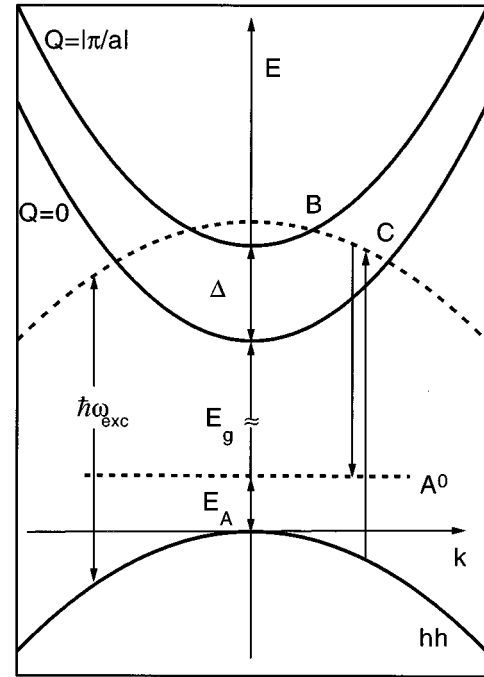


FIG. 2. Schematic representation of the optical transitions involved in $1hh \rightarrow 1e \rightarrow A^0$ HEL in a SL. The arrow pointing upwards (length $\hbar\omega_{\text{exc}}$) corresponds to the excitation of electrons from the heavy-hole subband (hh parabola) to the electron miniband. Possible transitions for different values of lateral momentum k occur between points B and C . The arrow pointing downwards corresponds to the HEL recombination with an A^0 acceptor state. See text for details.

Appendix A]. The photogenerated hot electrons recombine with acceptor-bound holes ($1e \rightarrow A^0$). The parabolas for fixed miniband wave vectors $Q = \pm \pi/a$ and $Q=0$ in Fig. 2 represent the dependence of E on lateral momentum k for the upper and lower edges of the electron miniband, respectively. A family of parabolas located between these two extrema corresponds to intermediate points of the miniband with $0 < |Q| < \pi/a$.

The lowest-energy parabola in Fig. 2 shows the heavy-hole dispersion, neglecting the valence band warping. The dashed parabola is obtained by adding the excitation energy $\hbar\omega_{\text{exc}}$ to the hole dispersion. The region where the dashed curve crosses a band of electron states (between points B and C) determines possible electron states which can be excited by photons $\hbar\omega_{\text{exc}}$. Every state of this band is characterized by the total kinetic energy E and the lateral momentum $\hbar k$. In the process of recombination an electron with $E(k, Q)$ emits a photon with a polarization $\rho_l^{\text{SL}}(k, Q)$ which strongly depends on the value of k .

We assume that the matrix elements of optical transitions in a SL are the same as in a QW (see Appendix A). This approximation is valid as long as the miniband width is smaller than the confinement energy. Thus the polarization in a SL can be expressed as $\rho_l^{\text{SL}}(k, Q) = \rho_l^{\text{QW}}(E_k)$, the HEL polarization for electrons with lateral kinetic energy E_k in an isolated QW which increases with increasing E_k .⁹ At the upper edge of the electron miniband (point B in Fig. 2) the energy of lateral motion is $E_k = E - \Delta$. Thus the energy de-

pendence of the linear polarization at point *B* may be expressed as

$$\rho_l^{SL}(E) = \begin{cases} \rho_l^{QW}(0) = 0, & \text{at } E < \Delta \\ \rho_l^{QW}(E - \Delta), & \text{at } E > \Delta. \end{cases} \quad (5)$$

This expression explains the peculiarities in the energy dependence of $\rho_l(E)$ presented in Fig. 1(a). In accordance with Eq. (5), $\rho_l(E)$ tends to zero at an energy which is approximately equal to the miniband width of $\Delta = 100$ meV for the (40/6) Å SL and $\Delta = 30$ meV for the (40/14) Å SL.

It follows from Eq. (5) that the electrons with minimal *k* (point *B* in Fig. 2) make the main contribution to the intensity of the zero-phonon HEL peak. This assumption is supported by the following reasons. First of all, the matrix elements of the $1e \rightarrow A^0$ transitions decrease with increasing *k* because the wave function of the acceptor-bound hole in the momentum representation drops very rapidly with increasing lateral wave vector. Secondly, the matrix element of the $1\text{hh} \rightarrow 1e$ transition also decreases with increasing *k*.¹⁰ Finally, the contribution of electrons with minimal *k* is further enhanced due to the singularity of the one dimensional density of states at $Q = \pm \pi/a$. This creates the possibility of momentum-selective optical alignment of photogenerated electrons. Electrons excited with an energy $E = \Delta$ mainly propagate along the miniband axis, while electrons with $E > \Delta$ move predominantly in the SL plane. In other words, the higher the electron energy the closer is their momentum distribution function to that observed in a QW. Note that this effect can also be used to determine the SL miniband width.

Figure 1(b) shows the energy dependence of the circular polarization ρ_c measured in the same samples. Contrary to the linear polarization, ρ_c decreases with increasing energy in QW's⁹ in accordance with theoretical predictions.¹⁰ In SL's one expects ρ_c to be constant and maximum [$\rho_c^{SL}(E) = \rho_c^{QW}(0)$] for energies $E < \Delta$, while in a QW it should decrease with increasing kinetic energy [$\rho_c^{SL}(E) = \rho_c^{QW}(E - \Delta)$ for $E > \Delta$]. Such behavior is observed for the (40/14) Å and (40/6) Å samples in Fig. 1(b).

2. Polarization distribution across the zero-phonon peak

Figure 3 displays the intensity (dotted lines) and polarization (circles) distribution across the zero-phonon peak of the (40/80) Å MQW [Fig. 3(c)] and the (40/6) Å SL (miniband width $\Delta = 100$ meV) for two different excitation energies [Fig. 3(a), 3(b)]. For the SL these energies were chosen to excite electrons with kinetic energies $E \approx \Delta$ [Fig. 3(a)] and $E \approx 2\Delta$ [Fig. 3(b)], respectively. If the electron kinetic energy substantially exceeds the SL electron miniband width ($E \approx 2\Delta$) the HEL polarization distribution [Fig. 3(b)] becomes very similar to that of a QW [Fig. 3(c)]. The polarization distribution changes strongly when the kinetic energy of photogenerated electrons exceeds the miniband width only slightly [$E \approx \Delta$, Fig. 3(a)]. Figure 3(a) shows that the polarization of electrons at the high energy side of the peak is close to zero. With decreasing *E* it reaches a maximum of $\rho_l = 0.11$ and then drops again.

The width of the zero-phonon peak (in the process $\text{hh} \rightarrow e \rightarrow A^0$) in bulk and QW samples is caused by the warping of the heavy-hole subband as well as by inhomogeneous

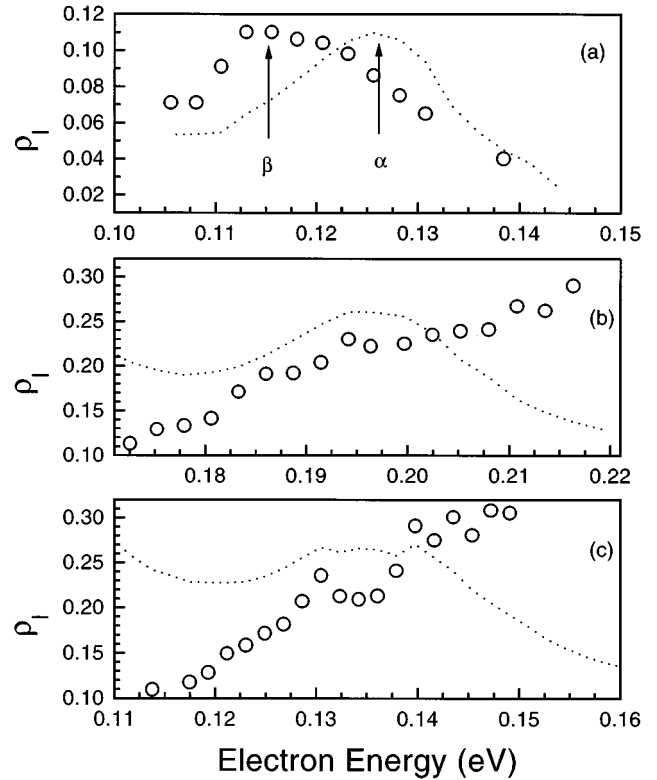


FIG. 3. Intensity (dotted lines) and linear polarization ρ_l (circles) vs hot electron energy across the zero-phonon HEL peak of a (40/6) Å SL (miniband width $\Delta = 100$ meV) for two different excitation energies $\hbar\omega_{\text{exc}}^1 = 1.833$ eV ($E \approx \Delta$) (a) and $\hbar\omega_{\text{exc}}^2 = 1.916$ eV ($E \approx 2\Delta$) (b) and for a (40/80) Å MQW (c). The arrows labeled α and β in (a) mark the points where the effect of a magnetic field on the linear polarization was studied (see Figs. 5 and 6)

broadening of the acceptor states. The heavy-hole subband warping in a QW produces a width in the initial energy distribution given by

$$\Delta E \sim m_c \left(\frac{1}{m_{[100]}} - \frac{1}{m_{[110]}} \right) (\hbar\omega_{\text{exc}} - E_g). \quad (6)$$

Here m_c is the electron effective mass, $m_{[100]}$ and $m_{[110]}$ are the heavy-hole masses in the [100] and [110] directions, respectively. We assume that $m_c \ll m_{[100]} < m_{[110]}$, consistent with known band structure parameters. The energy interval ΔE determines the width of the zero-phonon peak if electrons recombine with monoenergetic acceptor states.

Thus the low and high energy edges of the zero-phonon peak correspond to electrons excited with lateral wave vectors $\mathbf{k} \parallel \{100\}$ and $\mathbf{k} \parallel \{110\}$, respectively. If excitation of the HEL takes place in the configuration $\mathbf{e}_{\text{exc}} \parallel [110]$ the electrons with $\mathbf{k} \parallel \{100\}$ are not aligned and consequently the low frequency edge of the zero-phonon peak will be unpolarized. Conversely, electrons with $\mathbf{k} \parallel \{110\}$ contribute to the high energy edge of the zero-phonon peak and their recombination should be polarized. Therefore one expects the polarization to grow from the low frequency edge to the high frequency one, as observed experimentally for the (40/80) Å MQW [see Fig. 3(c)].

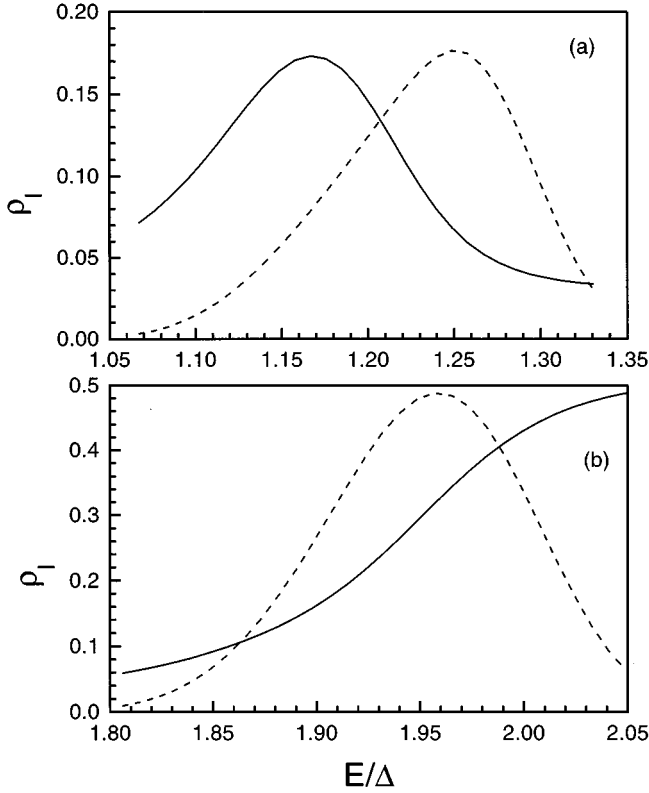


FIG. 4. Calculated distribution of the intensity (dashed line) and polarization ρ_l (solid line) across the zero-phonon HEL peak of a (40/6) Å SL for two different electron energies $E \approx \Delta$ ($\hbar\omega_{\text{exc}}^1 = 1.833$ eV) (a) and $E \approx 2\Delta$ ($\hbar\omega_{\text{exc}}^2 = 1.916$ eV) (b).

In a SL the existence of a miniband causes an additional broadening of the peak. One can see in Fig. 2 that photons with energy $\hbar\omega_{\text{exc}}$ generate electrons in the $B-C$ energy interval whose width is given by

$$\Delta E \sim \frac{m_c}{m_v} \Delta. \quad (7)$$

If the hole warping is neglected the high-energy edge of the zero-phonon peak is formed by electrons with minimum lateral energy (point B in Fig. 2) resulting in a low degree of polarization. On the other hand, electrons with maximum lateral energy (point C) and high alignment contribute to the low-energy edge. One should therefore expect the polarization to increase from the high energy edge to the low energy one because of the increase in the lateral energy. Thus warping and miniband width have opposite effects on the polarization distribution across the peak. The competition of these two effects explains the nonmonotonic dependence of the polarization across the zero-phonon peak displayed in Fig. 3(a). Comparison of Eqs. (6) and (7) shows that the miniband effect dominates at low excitation energies and that the role of warping increases with increasing $(\hbar\omega_{\text{exc}} - E_g)$. The experimental results in Figs. 3(a) and 3(b) are in accordance with these considerations.

Figure 4 presents the calculated intensity (dashed lines) and polarization (solid lines) distribution across the zero-phonon peak. In this model calculation we used the transition matrix elements and the heavy-hole dispersion for a single

40 Å QW, taking into account the warping and the complex structure of the valence band. The electron miniband was calculated in the tight binding approximation (see Appendix A). In order to evaluate the matrix element of the $1e \rightarrow A^0$ transition the wave function of the acceptor-bound hole was assumed to be composed of heavy-hole Bloch states. The Bohr radius of the acceptor was set equal to 20 Å. The results were smoothed by a Gaussian distribution with a width of 10 meV which simulates the spread of the acceptor levels. Calculations were made for two initial electron energies $E \approx \Delta$ [Fig. 4(a)] and $E \approx 2\Delta$ [Fig. 4(b)], corresponding to those used in the experiment [Figs. 3(a) and 3(b)]. The comparison of Figs. 3 and 4 shows that there is qualitative agreement between the experimental and theoretical results. We conjecture that the quantitative differences in the absolute values of ρ_l are caused by inaccuracies of the model used for the calculation of the acceptor states.

B. The HEL polarization in a magnetic field

We have investigated the dependence of the linear and circular HEL polarization on magnetic field in the Faraday ($\mathbf{B} \parallel \mathbf{n} \parallel z \parallel [001]$) and Voigt ($\mathbf{B} \perp \mathbf{n} \parallel z \parallel [001]$) geometries. In the Farady geometry the electric field of the light (propagation direction \mathbf{n} , SL growth direction z) was directed along the $[110]$ crystal axis and was thus perpendicular to the magnetic field. In the Voigt geometry the electric field of the laser field was either parallel ($\mathbf{B} \parallel \mathbf{e}_{\text{exc}}$) or perpendicular ($\mathbf{B} \perp \mathbf{e}_{\text{exc}}$) to the magnetic field, however, in both cases $\mathbf{e}_{\text{exc}} \parallel [110]$.

In the Faraday geometry the magnetic field leads to a decrease of the linear polarization. Similar to the bulk^{1,3} and QW's,^{5,6} this decrease of ρ_l in a SL follows the Lorentz function $\rho_l(B) = \rho_l(0) / [1 + (B/B_{1/2})^2]$, where $B_{1/2}$ is the magnetic field at which ρ_l decreases to one half of the initial value. The value of $B_{1/2}$ was about 3.5 – 4 T in all samples studied.

In the Faraday geometry no influence of the magnetic field on the circular HEL polarization was detected. The same behavior has been observed in QW's,⁵ while in bulk samples the circular polarization depends strongly on the magnetic field.¹¹ This fact demonstrates the absence of spin-momentum correlation in a SL, similar to the situation in QW's.

1. Magnetic field dependence of the linear HEL polarization under linearly polarized excitation in the Voigt geometry

In the Voigt geometry in a SL (contrary to a QW) the magnetic field affects the linear polarization. Figures 5(a) and 5(b) show the magnetic field dependence of ρ_l for the zero-phonon peak at electron energies $E \approx \Delta$ (circles) and $E \approx 2\Delta$ (triangles) in the (40/6) Å SL. For $E \approx \Delta$ the measurements were made at two different points of the zero-phonon peak marked in Fig. 3(a) as α (maximum of the peak) and β (maximum of the polarization). The data in Fig. 5(a) are for the α point, those in Fig. 5(b) for the β point. Open (filled) symbols in Figs. 5(a) and 5(b) are for the excitation polarized perpendicular (parallel) to \mathbf{B} .

Let us first discuss the magnetic field effect on the polarization in a SL when the kinetic energy of the photogenerated electrons is similar to the miniband width, i.e., $E \approx \Delta$

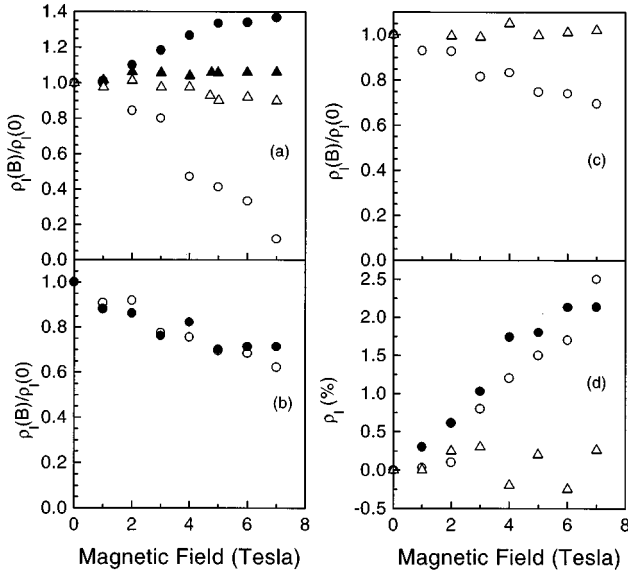


FIG. 5. Magnetic field dependence of the linear polarization ρ_l in the Voigt geometry: (a) for a (40/6) Å SL at the zero-phonon HEL peak. The open and filled circles represent measurements at an electron energy $E \approx \Delta$ [α point in Fig. 3(a)], while the open and filled triangles show data at $E \approx 2\Delta$; (b) ρ_l for the same SL at the β point in Fig. 3(a) (electron energy $E \approx \Delta$); (c) for bulk GaAs (open circles) and a (40/80) Å MQW (open triangles). In (a), (b), and (c) the filled symbols correspond to the $\mathbf{B} \parallel \mathbf{e}_{\text{exc}}$ configuration while the open ones are for $\mathbf{B} \perp \mathbf{e}_{\text{exc}}$; (d) magnetic field induced linear polarization under circularly polarized excitation in the (40/6) Å SL at $E \approx \Delta$ (open circles), in a bulk GaAs sample (filled circles), and in the (40/80) Å MQW (open triangles).

[circles in Figs. 5(a) and 5(b)]. This effect can be understood if one considers the change of wave vector k in a SL with magnetic field. In a QW a magnetic field applied in the plane cannot change the k vector if the cyclotron radius is larger than the well width and ρ_l remains constant.⁶ Data in Fig. 5(c) (open triangles) for a (40/80) Å MQW show that this is the case for the present experimental conditions where $B \leq 7$ T. In a SL the electron kinetic energy E depends on the lateral wave vector \mathbf{k} as well as the miniband wave vector Q . A magnetic field does not affect k_{\parallel} , the projection of \mathbf{k} on \mathbf{B} . However, it changes k_{\perp} , the projection of \mathbf{k} on the plane perpendicular to \mathbf{B} , and Q in such a way that the total energy E is conserved.

It has been pointed out above that in the tight binding approximation (see Appendix A) the matrix elements of optical transitions in a SL do not depend on the miniband wave vector Q , and for a fixed lateral \mathbf{k} they are the same as in a QW. This means that momentum alignment and linear polarization in a SL are determined only by the electron lateral momentum, like in a QW. Thus, the changes in the linear polarization are caused by the influence of a magnetic field on k_{\perp} . At the same time the changes of Q in a magnetic field do not affect ρ_l . In other words, in a SL the value $\langle k_z^2 \rangle$ in Eqs. (2) and (4) does not depend on Q and coincides with that in a QW.

The experimental findings in Fig. 5(a) (open and filled circles) may be explained as follows. Electrons with the lowest k make the main contribution to the intensity of the zero-

phonon peak (point B in Fig. 2). The miniband kinetic energy of these electrons is maximum and in a magnetic field it can only decrease. At the same time the lateral kinetic energy ($\propto k_{\perp}^2$) increases because the total energy has to be conserved. In other words, the magnetic field transforms the miniband motion into lateral motion. If a magnetic field is parallel to the electric field vector of the exciting light ($\mathbf{B} \parallel \mathbf{e}_{\text{exc}} \parallel x$) k_y^2 in Eq. (2) may be substituted by k_{\perp}^2 and k_x^2 by k_{\parallel}^2 . Thus, in accordance with Eq. (2), one should expect ρ_l to increase as is experimentally observed for this configuration [see filled circles in Fig. 5(a)]. In the other case ($\mathbf{B} \perp \mathbf{e}_{\text{exc}} \parallel x$) $k_x^2 = k_{\perp}^2$, and $k_y^2 = k_{\parallel}^2$ should be substituted in Eq. (2). The analysis of Eq. (2) shows that in this configuration ρ_l drops with increasing magnetic field, in general agreement with the experiment [open circles in Fig. 5(a)].

It was demonstrated in Sec. III A 2 that the lateral kinetic energy of the photogenerated electrons contributing to the zero-phonon HEL peak differs substantially throughout the peak, increasing from the higher- to the lower-energy edge. A magnetic field can now either increase or decrease k_{\perp}^2 . Thus, in accordance with Eq. (2), the magnetic field dependence of ρ_l can be steeper than that observed at the α point or even inverse. To check this prediction we measured the magnetic field dependence of ρ_l at the β point [open and filled circles in Fig. 5(b)], which is mostly due to the luminescence of electrons with maximum lateral kinetic energy (i.e., point C in Fig. 2). The polarization ρ_l in the ($\mathbf{B} \parallel \mathbf{e}_{\text{exc}}$) configuration [filled circles in Fig. 5(b)] decreases with magnetic field contrary to the dependence at the α point [filled circles in Fig. 5(a)]. The magnetic field induced reduction of ρ_l in the ($\mathbf{B} \perp \mathbf{e}_{\text{exc}} \parallel x$) geometry [open circles in Fig. 5(b)] is weaker at the β point than at the α point [open circles in Fig. 5(a)].

Figure 6 shows the magnetic field dependence of ρ_l calculated for two points of the zero-phonon peak of the (40/6) Å SL of Figs. 3(a) and 4(a), corresponding to electron energies of $E = 1.25\Delta$ [Fig. 6(a)] and 1.21Δ [Fig. 6(b)]. The dependence calculated for two polarization configurations (solid line: $\mathbf{B} \parallel \mathbf{e}_{\text{exc}}$, dashed line: $\mathbf{B} \perp \mathbf{e}_{\text{exc}}$) at the maximum of the zero-phonon peak [α point of Fig. 3(a)] is presented in Fig. 6(a), while similar curves for its low-energy tail [β point of Fig. 3(a)] are shown in Fig. 6(b). The calculations were made with the same model used for calculating the polarization distribution across the zero-phonon peak in Fig. 4(a) (see Appendix B). Within this model the time dependence of the \mathbf{k} vector in a magnetic field follows Eqs. (B1) and (B2) of Appendix B. The intensity of radiation emitted by an electron with wave vector $\mathbf{k}(t)$ was averaged over time with a statistical weight $(1/\tau)\exp(-t/\tau)$, where $1/\tau$ is the rate of LO phonon emission. The experimental and calculated magnetic field dependences presented in Figs. 5(a),(b) and Figs. 6(a),(b) agree well with each other [compare the open and filled circles in Fig. 5(a) with the solid and dashed lines in Fig. 5(a) as well as the open and filled circles of Fig. 5(b) with the solid and dashed lines in Fig. 6(b)].

With increasing electron energy, i.e., with an increase of the ratio E/Δ , the magnetic field effect on the linear polarization in Voigt geometry decreases and the situation becomes similar to that of an isolated QW. This is clearly demonstrated in Fig. 5(a) which, in addition to data of $E \approx \Delta$,

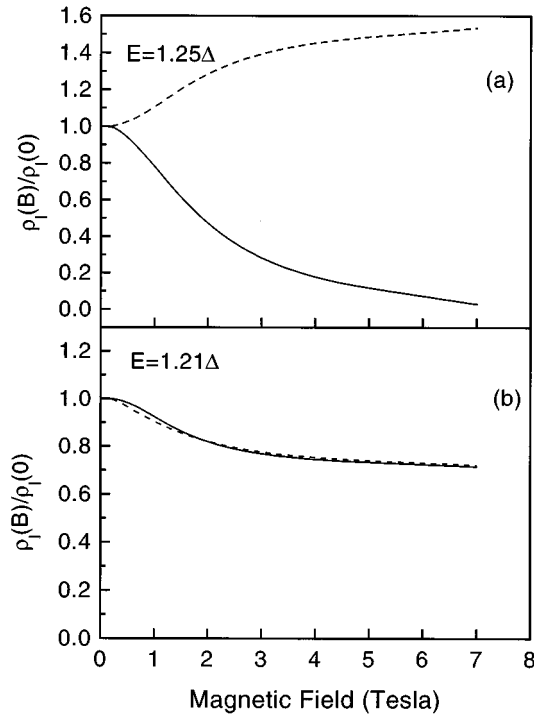


FIG. 6. Magnetic field dependence of the linear polarization ρ_l in the Voigt geometry calculated for two points of the zero-phonon HEL peak of the (40/6) Å SL shown in Figs. 3(a) and 4(a). The electron kinetic energies of $E/\Delta = 1.25$ (a) and $E/\Delta = 1.21$ (b) correspond to the HEL maximum [α point in Fig. 3(a)] and its low-energy tail [β point in Fig. 3(a)]. The solid lines are for the $\mathbf{B} \perp \mathbf{e}_{\text{exc}}$ configuration while the dashed ones correspond to $\mathbf{B} \parallel \mathbf{e}_{\text{exc}}$.

also depicts the magnetic field dependence of ρ_l for the two polarization configurations $\mathbf{B} \perp \mathbf{e}_{\text{exc}} \parallel x$ (open triangles) and $\mathbf{B} \parallel \mathbf{e}_{\text{exc}} \parallel x$ (filled triangles) at $E \approx 2\Delta$. The magnetic field effect on ρ_l at $E \approx 2\Delta$ is considerably weaker than at $E \approx \Delta$: It is very close to the QW data given for comparison by the open triangles in Fig. 5(c) for a (40/80) Å system. This behavior is caused by the increase of the lateral momentum of photogenerated electrons with increasing energy. Away from the miniband, i.e., for lateral energies larger than Δ , changing the lateral momentum in a magnetic field by $\sim \sqrt{2m_c\Delta}$ is not important with respect to the total value of k . Therefore ρ_l remains almost unaffected by a magnetic field, both in SL's and QW's.

For comparison we also present in Fig. 5(c) the effect of a magnetic field on ρ_l in bulk GaAs (open circles) for the configuration with $\mathbf{B} \perp \mathbf{e}_{\text{exc}} \parallel x$ measured in the maximum of the zero-phonon HEL peak about 280 meV above the direct gap. As in a SL, ρ_l decreases with magnetic field due to the rotation of momentum aligned carriers under the Lorentz force.

In conclusion, the effect of a magnetic field on the linear polarization in a SL is similar to that in a bulk sample when the electron kinetic energy is close to the miniband width $E \approx \Delta$. It tends to that observed in QW's at higher electron kinetic energies.

2. The linear HEL polarization induced by a magnetic field in the Voigt geometry for circularly polarized excitation

To demonstrate more clearly the peculiarities of hot electron alignment in SL's we used the Voigt configuration and

circularly polarized excitation. Figure 5(d) shows how linear polarization appears in a magnetic field in this geometry. Two components of the HEL intensity parallel (I_{\parallel}) and perpendicular (I_{\perp}) to \mathbf{B} were measured. The linear polarization was calculated as discussed above (see Sec. III A). The open circles in Fig. 5(d) show the magnetic field induced linear polarization in a SL, while filled circles and open triangles present the same dependence for bulk GaAs and a MQW, respectively. The positive sign of the induced linear polarization means that the electric field vector of the HEL is predominantly parallel to \mathbf{B} , i.e., the wave vector of the excited electrons is predominantly perpendicular to \mathbf{B} . This result can be explained if one considers the dominant role played by electrons from the upper edge of the SL miniband in the formation of the zero-phonon peak. Circularly polarized excitation generates electrons with an axially symmetric momentum distribution. At $B=0$ the axis of symmetry in this configuration is directed along the miniband direction. Therefore the linear polarization in this geometry vanishes. In a magnetic field the decrease of the miniband energy of electrons is accompanied by an increase of their lateral kinetic energy, i.e., of k_{\perp}^2 . As a result, the momentum distribution function in a magnetic field is no longer axially symmetric and electrons with lateral k_{\perp} dominate. The recombination of electrons with such a momentum distribution function is partly linearly polarized, moreover the HEL is polarized predominantly parallel to the magnetic field.

The same effect is observed in bulk GaAs [see filled circles in Fig. 5(d)] where the momentum distribution function of electrons in bulk samples under circularly polarized excitation is axially symmetric with the axis perpendicular to \mathbf{B} .¹ The magnetic field rotates this distribution and produces an anisotropy in the plane perpendicular to the propagation direction of the exciting light \mathbf{n} . The wave vectors are directed predominantly perpendicular to the magnetic field. This magnetic field induced anisotropy is responsible for the appearance of the linear polarization. In a QW this effect cannot be observed as long as the cyclotron radius is larger than the well width. This is confirmed by the experimental results shown in Fig. 5(d) (open triangles).

IV. CONCLUSIONS

We have studied the effect of SL minibands on the HEL polarization and its dependence on magnetic field. The transition from a QW (2D system) to a SL (quasi-three-dimensional system) is accompanied by drastic changes in the HEL polarization which arise from a different dependence on the electron kinetic energy. The polarization in a SL tends to zero when the electron kinetic energy becomes equal to the miniband width, whereas in a QW zero polarization occurs at zero kinetic energy. This allows us to determine the SL miniband width by optical means. The linear polarization behavior in SL's is reproduced by tight binding calculations. Peculiarities of the quasi-three-dimensional electron motion, as compared to the 2D case, are most pronounced for a magnetic field in the Voigt geometry which transforms the miniband motion of electrons into motion in the SL plane. The shape of the momentum distribution function in a SL depends strongly on excitation energy and polarization. This property of the optical excitation in a SL can

be used for the generation of electrons with an anisotropic momentum distribution either along the miniband axis or in the SL plane, thus varying the propagation direction of photogenerated electrons. This nontrivial optical property of SL's may be useful for the design of new optoelectronic devices such as wavelength sensitive photodetectors.

ACKNOWLEDGMENTS

We thank I. I. Reshina and B. P. Zakharchenya for useful discussions and a critical reading of the manuscript. V.F.S., D.N.M., V.I.P., and A.Yu.D. acknowledge financial support from the Russian Fund of Basic Research (Grant Nos. 96-02-16895 and 95-02-04055) and the Volkswagen Foundation (Grant No. I/70958). V.F.S. thanks the Max-Planck-Gesellschaft for financial support and the Max-Planck-Institut für Festkörperforschung for hospitality. Thanks are due to B. Koopmans for a critical reading of the manuscript.

APPENDIX A: MATRIX ELEMENTS OF OPTICAL TRANSITIONS IN THE TIGHT BINDING APPROXIMATION

In order to describe electron states in the conduction band of a SL we use the tight binding approximation with the wave functions:

$$\Psi_{\mathbf{k}Q}(\boldsymbol{\rho}, z) = \frac{1}{\sqrt{N}} e^{i\mathbf{k}\boldsymbol{\rho}} \sum_n e^{iQz_n} \psi(z - z_n), \quad (\text{A1})$$

where $\boldsymbol{\rho}$ and z are the coordinates in and perpendicular to the QW planes, $z_n = na$ are the coordinates of well centers, a is the SL period, $\psi(z)$ is the wave function in a single QW, and N is the number of wells in a SL. The electron energy in this state is represented by

$$E(k, Q) = \frac{\hbar^2 k^2}{2m_c} + \frac{\Delta}{2} (1 - \cos Qa), \quad (\text{A2})$$

where Δ is the miniband width. The hole wave function can be expressed in a way similar to A1. Two types of terms appear in the calculation of the matrix elements of the optical transitions. The first term corresponds to the recombination (or generation) of an electron and a hole localized in the same well, the second term to hole and electron localized in

different QWs. In the tight binding approximation the terms of the second type cause only small corrections to the matrix elements. These modifications result from the overlap of the electron and hole wave functions in neighboring wells. If these corrections are neglected, the matrix elements of interband transitions do not depend on the miniband wave vector Q and for a fixed lateral wave vector \mathbf{k} they are the same as for the isolated QW. However, the existence of minibands can strongly affect the HEL polarization because electrons with a fixed total kinetic energy E can have very different lateral kinetic energies. This is especially important when the total kinetic energy E is close to or smaller than the miniband width.

APPENDIX B: ELECTRON MOTION IN k SPACE IN A MAGNETIC FIELD

A magnetic field applied along the growth direction of a SL rotates the lateral vector \mathbf{k} as in an isolated QW but it does not affect the miniband wave vector Q . The effects of a magnetic field on electron momentum in a SL and a QW differ drastically when the magnetic field is applied in the plane of the SL (QW). In this geometry the lateral component k_{\parallel} (along \mathbf{B}) does not depend on the magnetic field, while k_{\perp} (perpendicular to \mathbf{B}) and the miniband wave vector Q change in time in such a way that the total energy is conserved. From the usual equations of motion

$$\frac{d\mathbf{p}}{dt} = \frac{e}{c} [\mathbf{v} \times \mathbf{B}], \quad \mathbf{v} = \frac{\partial E}{\partial \mathbf{p}}; \quad \mathbf{p} = (\hbar \mathbf{k}, \hbar Q),$$

one can obtain using Eq. (A2)

$$\frac{dQ}{dt} = \omega_c k_{\perp}, \quad \frac{dk_{\perp}}{dt} = -\frac{\eta^2 \omega_c}{a} \sin Qa, \quad (\text{B1})$$

where $\eta^2 = \Delta m_c a^2 / 2\hbar^2$, $\omega_c = |e|B/m_c c$. These equations can be converted into the pendulum equation

$$\frac{d^2 \theta}{dt^2} = -\omega_c^2 \eta^2 \sin \theta, \quad (\text{B2})$$

where $\theta = Qa$ is the angle of deviation of the pendulum from the vertical direction. The transverse component of wave vector, k_{\perp} , can be obtained from the angular velocity of the pendulum as $k_{\perp} = \omega_c^{-1} a^{-1} d\theta/dt$.

¹B. P. Zakharchenya, D. N. Mirlin, V. I. Perel', and I. I. Reshina, *Usp. Fiz. Nauk* **136**, 459 (1982) [*Sov. Phys. Usp.* **25**, 143 (1982)].

²S. A. Lyon, *J. Lumin.* **35**, 121 (1986).

³M. A. Alekseev, I. Ya Karlik, D. N. Mirlin, and V. F. Sapega, *Fiz. Tekh. Poluprovodn.* **23**, 761 (1989) [*Sov. Phys. Semicond.* **23**, 479 (1989)].

⁴D. N. Mirlin and V. I. Perel', *Semicond. Sci. Technol.* **7**, 1221 (1993).

⁵B. P. Zakharchenya, P. S. Kop'ev, D. N. Mirlin, D. G. Polyakov, I. I. Reshina, V. F. Sapega, and A. A. Sirenko, *Solid State Commun.* **69**, 203 (1989).

⁶P. S. Kop'ev, D. N. Mirlin, D. G. Polyakov, I. I. Reshina, V. F.

Sapega, and A. A. Sirenko, *Fiz. Tekh. Poluprovodn.* **24**, 1200 (1990) [*Sov. Phys. Semicond.* **24**, 1200 (1990)].

⁷J. A. Kash, M. Zachau, M. A. Tischler, and U. Ekenberg, *Phys. Rev. Lett.* **69**, 2260 (1992).

⁸M. Zachau, J. A. Kash, and W. T. Masselink, *Phys. Rev. B* **44**, 4048 (1991).

⁹D. N. Mirlin, V. F. Sapega, A. A. Sirenko, M. Cardona, and K. Ploog, *Fiz. Tekh. Poluprovodn.* **27**, 990 (1993) [*Sov. Phys. Semicond.* **27**, 537 (1993)].

¹⁰I. A. Merkulov, V. I. Perel', and M. E. Portnoi, *Zh. Éksp. Teor. Fiz.* **99**, 1202 (1990) [*Sov. Phys. JETP* **72**, 669 (1990)].

¹¹I. Ya. Karlik, D. N. Mirlin, L. P. Nikitin, D. G. Polyakov, V. F.

- Sapega, Pis'ma Zh. Éksp. Teor. Fiz. **36**, 155 (1982) [JETP Lett. **36**, 192 (1992)].
- ¹²V. F. Sapega, V. I. Perel', A. Yu. Dobin, D. N. Mirlin, I. A. Akimov, T. Ruf, M. Cardona, and K. Eberl, Pis'ma Zh. Éksp. Teor. Fiz. **63**, 285 (1996) [JETP Lett. **63**, 305 (1996)].
- ¹³V. F. Sapega, V. I. Perel', A. Yu. Dobin, D. N. Mirlin, I. A. Akimov, T. Ruf, M. Cardona, and K. Eberl, in *Proceedings of the 23rd International Conference on the Physics of Semiconductors*, edited by M. Scheffler and R. Zimmermann (World Scientific, Singapore, 1996), p. 1711.